ARL 67-0185
SEPTEMBER 1967

Aerospace Research Laboratories

NOSE BLUNTNESS, CONE ANGLE, AND MACH NUMBER EFFECTS ON THE STABILITY DERIVATIVES OF SLENDER CONES

JAMES T. CLAY, MAJOR, USAF
HYPERSONIC RESEARCH LABORATORY

Project No. 7064

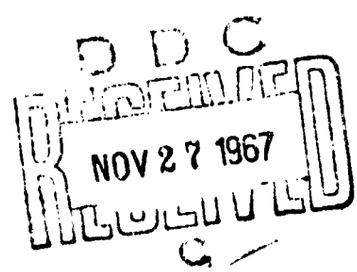

OFFICE OF AEROSPACE RESEARCH
United States Air Force

46

NOTICES

When Government drawings, specifications, or other data are used for any purpose other than in connection with a definitely related Government procurement operation, the United States Government thereby incurs no responsibility nor any obligation whatsoever; and the fact that the Government may have formulated, furnished, or in any way supplied the said drawings, specifications, or other data, is not to be regarded by implication or otherwise as in any manner licensing the holder or any other person or corporation, or conveying any rights or permission to manufacture, use, or sell any patented invention that may in any way be related thereto.

Agencies of the Department of Defense, qualified contractors and other government agencies may obtain copies from the

Defense Documentation Center
Cameron Station
Alexandria, Virginia 22314

This document has been released to the

- - - - - - - - - -

CLEARINGHOUSE
U.S. Department of Commerce
Springfield, Virginia 22151

for sale to the public.

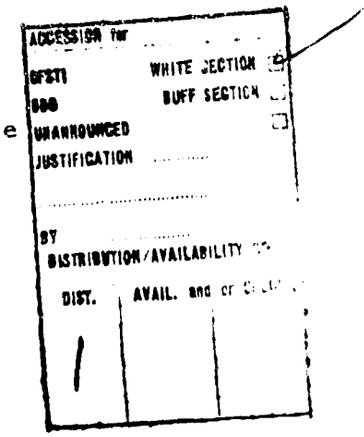

Copies of ARL Technical Documentary Reports should not be returned to Aerospace Research Laboratories unless return is required by security considerations, contractual obligations or notices on a specified document.

300 - November 1967 - CO455 - 13-264

ARL 67-0185

NOSE BLUNTNESS, CONE ANGLE, AND MACH NUMBER EFFECTS ON THE STABILITY DERIVATIVES OF SLENDER CONES

JAMES T. CLAY, MAJOR, USAF

HYPERSONIC RESEARCH LABORATORY

SEPTEMBER 1967

Project 7064

AEROSPACE RESEARCH LABORATORIES
OFFICE OF AEROSPACE RESEARCH
UNITED STATES AIR FORCE
WRIGHT-PATTERSON AIR FORCE BASE, OHIO

FOREWORD

This report, prepared by James T. Clay of the Hypersonic Research Laboratory, Aerospace Research Laboratories, is a contribution to a study of hypersonic stability problems under Project 7064, entitled "High Velocity Fluid Mechanics."

The author gratefully acknowledges the advice given by Mr. O. Walchner during the course of this study. The competent assistance in instrumentation and data acquisition given by Mr. Frank Sawyer, the support in wind tunnel operation given by the staff of the Fluid Dynamics Facilities Research Laboratory, and the assistance in preparing this report given by the secretaries of the Hypersonic Research Laboratory are all greatly appreciated.

ABSTRACT

A theoretical and experimental study to evaluate the influence of spherical nose bluntness, of cone angle, c. g. location and Mach number on the stability characteristics in pitch of blunt slender cones has been conducted at the USAF Aerospace Research Laboratories. A 10° half-angle cone with nose bluntness ratios from .025 to .30 was investigated in the ARL 20" Hypersonic Wind Tunnel at M = 14. The small amplitude free oscillation technique was used to extract the static and dynamic stability derivatives from the time history of a planar oscillatory motion about zero trim angle of attack. The observed effect of the nose bluntness on the stability derivatives was quite similar to earlier results with a 5.6° half-angle cone. Again, a severe breakdown of the damping derivatives was found for large bluntness ratios. An estimate of the pitch-induced angles of attack for large bluntness ratios was based on the physics of the blast wave type flow. It was found that these induced angles differ from those applicable for pointed cones or for small bluntness ratios where the flow has mainly conical character. The tangent cone method in connection with these different types of pitch-induced angles of attack qualitatively predicts the observed breakdown of the damping derivatives. A computer program designed by General Electric Corp. was used to compare the ARL test results with G. E.'s unsteady flow field theory. Reasonably good agreement was obtained. The G. E. program was also used to calculate the effects of cone angle, c. g. location, and Mach number on the stability derivatives of spherically blunted cones. The earlier derived parameter $C = \sqrt{\Theta_c (1-\xi)/2\xi}$ was found, to correlate well the effect of nose blunting on the stability derivatives, (Θ_c = cone half angle, ξ = nose radius/base radius).

TABLE OF CONTENTS

LIST OF ILLUSTRATIONS

NOMENCLATURE

C = $\sqrt{\Theta_c (1-\xi)/2\xi}$, cone angle-bluntness ratio correlation parameter

C_m = $\frac{M}{q_\infty SL}$, pitching moment coefficient

C_{m_α} = $\frac{\partial C_m}{\partial \alpha}$, static pitching moment derivative

$C_{m_q} + C_{m_{\dot{\alpha}}}$ = $\frac{\partial C_m}{\partial \left(\frac{qL}{U_\infty}\right)} + \frac{\partial C_m}{\partial \left(\frac{\dot{\alpha} L}{U_\infty}\right)}$, damping moment derivatives

C_p = $\frac{p - p_\infty}{q_\infty}$, pressure coefficient

C_{D_N} = $\frac{\text{Nose Drag}}{q_\infty \left(\frac{\pi d^2}{4}\right)}$, nose drag coefficient

d = nose diameter, ft.

f = time frequency, cyc/sec

I = transverse moment of inertia, slug ft^2

K = $M_\infty \tan \Theta_c$, hypersonic similarity parameter

ℓ = model length measured from center of nose, ft.

L = total model length, ft.

M = pitching moment about center of gravity, ft-lb, also Mach number

n = $\frac{Cp}{2\Theta_c^2}$, blunt cone pressure function

p = surface pressure, lb/ft^2

p_0 = free stream stagnation pressure, psia

q = pitching velocity, rad/sec

q_∞ = $\frac{\rho}{2} U_\infty^2$, dynamic pressure, lb/ft^2

r = nose radius, ft

R = base radius, ft

R_{cg} = radius of the flight path of the center of gravity, ft

$S = R^2\pi$ = reference area, ft^2

T_0 = free stream stagnation temperature, °R

U_∞ = free stream velocity, ft/sec

x = distance along model centerline measured from stagnation point, ft

x' = distance along model centerline measured from center of radius of nose, ft

x_{cg} = center of gravity location, ft

α = static angle of attack, rad

α_{eff} = local effective angle of attack induced by rotation, rad

γ = ratio of specific heats

δ = $\frac{1}{i} \ln \frac{\alpha_1}{\alpha_i}$, log decrement, i is the number of the cycle being considered

ϵ = $\frac{\gamma - 1}{\gamma + 1}$

ξ = $\frac{r}{R}$, nose bluntness ratio

Θ_c = cone half angle, deg

ρ = free stream density, slugs/ft^3

ω = $2\pi f$, circular frequency, rad/sec

INTRODUCTION

In recent years much emphasis has been placed on the study of the static and dynamic stability characteristics of both sharp and blunt slender cones in low and high Mach number flow[1, 3, 9, 17, 19]. Different approaches have been used to try to predict the stability derivatives of blunted cones. In Ref. 1 the tangent cone approximation was applied to the empirical blunt cone pressure distribution to obtain the stability derivatives of blunt cones at zero trim angle of attack. Reasonably good agreement was found between the theoretical and experimental static pitching moment derivatives over the entire range of nose bluntness ratios investigated. However, the damping derivatives were in reasonably good agreement for small bluntness ratios only, while the trends of analysis and experiment diverged for increasing nose bluntness ratios[2], i.e., for $C \lesssim 1$*. The experimentally observed reduction in the damping derivatives, $(C_{m_q} + C_{m_{\dot{\alpha}}})$, for a range of C values < 1 was, at first, thought to have been caused by boundary layer separation resulting from the adverse pressure gradient over the aft portion of the cone. This hypothesis was based on the earlier experience that a strong support interference can cause flow separation over a slender cone which, in turn, can induce dynamic instability.

Quinn[3] subsequently applied a perturbation technique to the blast wave-piston theory of Chernyi[4] to obtain the stability derivatives of blunt slender cones for $K \to \infty$. His analysis applies for values of $C < 0.5$ and qualitatively agrees well with the experiments at zero trim angle of attack, thus indicating that it is the blast wave effect of the high drag nose which causes the observed breakdown of the dynamic stability derivatives.

---

* The modified Cheng parameter of Ref. 1, $\Theta_c \sqrt{x/d}$, can be rewritten as $C\sqrt{x/l}$ where $C = \sqrt{\Theta_c (1-\xi)/2\xi}$.

The static and dynamic stability derivatives obtained from the tangent cone method depend on the input for the effective angle of attack. As for the static derivative, this input angle is the well-defined static angle of attack. For the damping derivative, it is the angle induced by the pitching motion. After the analysis of Ref. 3 was available, it was logical to speculate that the pitch-induced angles of attack may be different for the blast wave region and the conical flow regime. It will be shown in the following that this, indeed, is true. The tangent cone method in conjunction with these two different types of pitch-induced angles of attack furnishes derivatives which are qualitatively in agreement with earlier tests ($\Theta_c = 5.6°$) and with new tests ($\Theta_c = 10°$). The test results are also compared with the exact characteristics solution, known as G. E. Corp.'s unsteady flow field theory[9]. The observed agreement of numerical results and tests encouraged the use of this theory for a further study of the effects of Mach number, cone angle, and c.g. location for various bluntness ratios. It will be seen that the cone angle-bluntness ratio parameter C, as derived in Ref. 1, correlates well the effect of nose blunting on the static and dynamic stability derivatives.

ANALYSIS

An analysis for C_{m_q} will now be developed which explains why the analysis of Ref. 1 adequately predicts the damping derivatives for families of blunt slender cones defined by a value of $C \gtrsim 1$ but fails for $C < 1$[2]. For blunt slender cones, there are three different flow regimes to be considered, which are illustrated in Fig. 1. The parameter $\theta_c \sqrt{x/d}$ is used to set the limits of the flow regimes. This parameter is a modification of the original Cheng parameter, $(\theta_c^2/\sqrt{\epsilon\ C_{D_N}})\ (x/d)$, evaluated for $\gamma = 1.4$ and $C_{D_N} = 1.0$. The values chosen in Fig. 1 to limit the "blast wave" and "conical flow" regimes are somewhat arbitrary but are based upon the characteristics of the surface pressure over blunt slender cones and of the shock shape.

Let us first consider the blast wave region defined by $\theta_c \sqrt{x/d} \lesssim 0.5$. The shock wave stands far away from the body and has a power law shape. The layer of gas next to the body, termed the "entropy layer" has passed through the near normal portion of the shock and is characterized by high temperature, by low density, and by very little change in pressure in the radial direction. Between the "entropy layer" and the shock is concentrated the largest portion of the mass flow bounded by the shock. As is well known, a slight alteration of the body shape aft of a blunt nose and within the entropy layer has no appreciable effect on the shock shape. We will use this feature of the blast wave regime for an estimate of the pitch damping derivative C_{m_q} at zero trim angle of attack.

The derivative C_{m_q} defines the pitching moment due to a pitching motion with uniform pitching velocity, q, at constant angle of attack. Such a motion is realized by whirling the body on an arm around a fixed center through still air. The arm shall be connected to

the body at its c.g. and the velocity of the c.g. shall be U_∞.
Fig. 2a shows the arm perpendicular to the body axis, i.e., for zero angle of attack. The path of the c.g. is a circle with the radius $R_{cg} = U_\infty / q$. For any other station at the distance x' aft of the nose:

$$R_x = \sqrt{R_{cg}^2 + (x'_{cg} - x')^2} \approx R_{cg} \left[1 + \frac{1}{2} \left(\frac{x'_{cg} - x'}{R_{cg}} \right)^2 \right] \qquad (1)$$

Specifically for the nose:

$$R_N = R_{cg} \left[1 + \frac{1}{2} \left(\frac{x'_{cg}}{R_{cg}} \right)^2 \right] \qquad (2)$$

The circular path of the nose is "cambered" with respect to the body axis by

$$\Delta R = R_N - R_x = \frac{q}{U_\infty} \left[x'_{cg} x' - \frac{x'^2}{2} \right] \qquad (3)$$

In view of the very small curvature for $q\ell / U_\infty << 1$, we now assume that the curved shock is centered with respect to the circular path of the nose. We also assume that the radial extension of the shock downstream of the nose and the radial pressure distribution from shock toward the shock's centerline are the same as they would be for a rectilinear motion of the body.

Then, for a uniform pitching motion as shown in Fig. 2a, the shock is closer to the upper surface of the body by ΔR (x') than it would be in a rectilinear flight at zero angle of attack and further away from the lower surface by the same amount. Therefore, the pressures for the upper and lower surfaces are different. A local normal force and a corresponding elemental pitching moment result from this "eccentricity" of the shock relative to the body. For an estimate of this induced normal force we again use the analogy with rectilinear flight conditions. At the station x', the pitching body has the same

position relative to the shock wave as a nonpitching body in rectilinear flight at the angle of attack $\alpha = -\Delta R/x'$. If we assume that the local pressures on the upper and lower surface are the same in both cases, then the tangent cone method applied to the known zero lift-blunt cone surface pressure correlation, as outlined in Ref. 1, may be used to predict the resulting elemental pitching moment due to the uniform pitching motion. We, therefore, conclude that in the blast wave regime the effective local angle of attack due to a pure uniform pitching motion with zero trim angle of attack may be represented by

$$\alpha_{eff}(x') = -\Delta R/x' = \frac{q\ell}{U_\infty}\left[\frac{1}{2}\frac{x'}{\ell} - \frac{x'_{cg}}{\ell}\right], \Theta_c\sqrt{x/d} \lesssim .5 \qquad (4)$$

The "conical flow" regime is defined by $\Theta_c\sqrt{x/d} \gtrsim 0.8$. This is the region downstream of the blunt nose where the flow has completed the transition from blast wave type flow in the nose region to conical flow. The shock wave is conical in shape and lies close to the body. The shock angle and the surface pressure are essentially the same as for a pointed cone. In a whirling-arm motion the conical shock will remain with the rotating body, and from Fig. 2b it is seen that, for these conditions, the local effective angle of attack due to uniform pitching becomes

$$\alpha_{eff}(x') = \frac{x' - x'_{cg}}{R_{cg}} = \frac{q\ell}{U_\infty}\left[\frac{x'}{\ell} - \frac{x'_{cg}}{\ell}\right], \Theta_c\sqrt{x/d} \gtrsim .8 \qquad (5)$$

For the range $0.5 \lesssim \Theta_c\sqrt{x/d} \lesssim 0.8$, the flow undergoes the transition from blast wave flow to the conical flow, and neither of the models discussed above is valid.

The consequences of these different types of pitch induced local effective angles of attack can be seen from Fig. 3 where α_{eff} per unit of $q\ell/U_\infty$ is plotted versus x'/ℓ for $x'_{cg}/\ell = 0.4$. In the conical

flow regime, α_{eff} is negative in front of the c.g. and positive aft of the c.g. for a nose-up pitching motion ($q > 0$). The resulting negative and positive normal forces in front and aft of the c.g. respectively produce a moment which opposes the nose-up pitching motion and is therefore damping. For the blast wave regime, however, the portion in front of the c.g. produces a greater damping moment, while the portion aft of the c.g. produces a moment which is dynamically destabilizing for $(x'/\ell) < (2\, x'_{cg}/\ell)$ and stabilizing for $(x'/\ell) > (2\, x'_{cg}/\ell)$. Note, if $x'_{cg}/\ell > 0.5$, the whole rear portion produces a destabilizing moment.

In Ref. 1, the pitch damping derivative C_{m_q} was derived using the blunt cone-zero lift surface pressure correlation, as given in Ref. 6, and the tangent cone method to determine the local normal forces due to the local effective angle of attack given by equation (5). The resultant equation for C_{m_q} is

$$C_{m_q} = -\xi^2 \left(\frac{x'_{cg}}{\ell}\right)^2 - 4\int_0^1 \left[\frac{x'}{\ell}(1-\xi)^2 + \xi\,(1-\xi)\right]\left[\frac{x'}{\ell} - \frac{x'_{cg}}{\ell}\right]^2 \left[n + \frac{1}{2}\Theta_c \frac{\partial n}{\partial \Theta_c}\right] d\left(\frac{x'}{\ell}\right) \quad (6)$$

where $n = (C_p/2\Theta_c^2)$ represents the zero lift surface pressure correlation as a function of $\Theta_c \sqrt{x/d}$. However, from what is said before, the effective local angle of attack given by equation (4) should be more representative if the flow over the entire body is of the blast wave type, thus giving

$$C_{m_q} = -\xi^2 \left(\frac{x'_{cg}}{\ell}\right)^2 - 4\int_0^1 \left[\frac{x'}{\ell}(1-\xi)^2 + \xi\,(1-\xi)\right]\left[\frac{x'}{\ell} - \frac{x'_{cg}}{\ell}\right]\left[\frac{1}{2}\,\frac{x'}{\ell} - \frac{x'_{cg}}{\ell}\right] \times \left[n + \frac{1}{2}\Theta_c \frac{\partial n}{\partial \Theta_c}\right] d\left(\frac{x'}{\ell}\right) \quad (7)$$

Equation (7), therefore, applies for families of cones defined by $C \lesssim 0.5$.

If the flow over the rear portion is conical, then the effective local angle of attack over this portion due to pitching is given by equation (5). Applying this α_{eff} over the whole body, as was done in Ref. 1, would introduce erroneous local normal forces in the blast wave nose region and in the middle transition region. * However, the effects on C_{m_q} will be small, since the local normal forces are not only proportional to α_{eff} but are also proportional to the local cross-sectional area and for this reason are much smaller in the nose region than for the rear portion of a conical body. Also, the normal forces in the middle region make a small contribution to C_{m_q} because of the short lever arm with respect to the c.g. The main contribution to C_{m_q} is furnished by the rear portion; and the expression for C_{m_q}, given by equation (6), therefore, should give fair predictions for all blunt slender cones defined by a family parameter, $C \gtrsim 1.0$.

The empirical pressure derivative function, $(n + \frac{1}{2}\Theta_c(\partial n/\partial\Theta_c))$, of Ref. 1 was used to evaluate equations (6) and (7) for the 5.6° cone of Ref. 2 and the 10° cone reported herein, Fig. 4. The results are shown in Figs. 5b and 6b along with the experimental results discussed later in this report. Included are the results of the calculations using the G. E. flow field program[9] and the results of Quinn's blast wave analysis[3]. The new concept for the pitch-induced angles of attack, developed here, in conjunction with the tangent cone method, derived in Ref. 1, correctly predicts the trend of the experimental results for values of $C < 0.5$. The static derivatives are shown in Figs. 5a and 6a. It should be noted that in the experiments the pivot point of the flexure was fixed relative to the base of the cone, thus causing the x'_{cg}/ℓ to vary with nose bluntness ratio.

---

* e.g., for $C = 1.0$, the lower limit of the conical flow regime defined by $0.8 = \Theta_c\sqrt{x/d} = C\sqrt{x/\ell}$ is at the station $x/\ell = (.8/C)^2 = 0.64$; and the upper limit of the blast wave regime $0.5 = \Theta_c\sqrt{x/d} = C\sqrt{x/\ell}$ is at $x/\ell = .25$.

EXPERIMENT

A series of tests on a 10° blunt cone with bluntness ratios ranging from 0.025 to 0.30 were run in the ARL 20" Hypersonic Wind Tunnel. The results of these tests verify that the drastic reduction in damping derivatives observed for $\Theta_c = 5.6°$ also occurs for other cone angles, when the blast wave type flow becomes dominant, i.e., for $C < 1.0$.

A description of the wind tunnel and its operating ranges may be found in Refs. 11, 12, and 13. A nominal Mach number of 14.2 with $P_0 \approx 1215$ psia and $T_0 \approx 2000°R$ was used for these tests. Although the stagnation pressure and temperature used place the test core in a supersaturated state, tests by Daum[14] and Goddard[15] show there is a region of allowable supersaturation for this facility. The T_0 and P_0 for these tests placed us well within this region. Calibration of the nozzle used showed a maximum radial Mach number variation of $\pm$ 0.1 and an axial gradient of approximately 0.07 per foot.

The model and the free oscillation apparatus used for these tests were the same as those used in Ref. 10 except that the standard nose, $\xi = 0.0167$, was replaced with interchangeable noses with different bluntness ratios. A tabulation of the seven configurations tested is shown in Fig. 4.

The free oscillation technique with an initial displacement angle of approximately 2.8° was used. Only the zero trim angle of attack case was tested. As in Ref. 10, the time history of the model motion was obtained with an Optron Tracker and recorded with a Consolidated Electrodynamic Oscillograph. At least 200 cycles were obtained for each run.

The data were reduced using the equations for C_{m_α} and $(C_{m_q} + C_{m_{\dot{\alpha}}})$ of Ref. 16, which become

$$C_{m_\alpha} = -2\left(\frac{\omega_1 L}{U_\infty}\right)\left(\frac{I}{\rho SL^3}\right)\left[1 - \left(\frac{\omega_2}{\omega_1}\right)^2\right] \tag{8}$$

$$C_{m_q} + C_{m_{\dot{\alpha}}} = -\frac{2}{\pi}\left(\frac{\omega_1 L}{U_\infty}\right)\left(\frac{I}{\rho SL^3}\right)\left[\delta_1 - \left(\frac{\omega_2}{\omega_1}\right)^2 \delta_2\right] \tag{9}$$

when the nomenclature of this report is used. Note subscript 1 indicates wind-on conditions and subscript 2 indicates near vacuum wind-off conditions.

The results of these experiments are presented in Figs. 6a and 6b. In all cases except one, $\xi = 0.15$, there was no apparent effect of amplitude on the damping. However, for this bluntness ratio, which gives a value of $C = 0.704$, a definite reduction in the damping was observed as the amplitude of oscillation decreased. This might be attributed to the fact that the flow is more of a conical type for larger amplitudes of oscillation. Only one flexure was used giving reduced frequencies $\omega L/U_\infty = 0.0154$ to 0.0186 for the different models. The Reynolds numbers, referred to length and free stream conditions, were in the range from $.42 \times 10^6$ to $.55 \times 10^6$.

NUMERICAL CALCULATIONS

The reasonably good agreement between the experimental results and the results of the calculations made with the General Electric Corp. computer program[9] prompted a numerical experiment to investigate the influence of cone angle and Mach number on the stability derivatives. This program, designed for the IBM 7094 computer, used a flow field approach combined with small perturbation techniques to obtain the pressure and the appropriate derivatives of the pressure acting on axisymmetric or two dimensional bodies in supersonic flow. These derivatives are then integrated over the surface of the body to obtain the stability derivatives. The following table lists the configurations for which calculations were made.

Θ_c	Mach Number	$\frac{x_{cg}}{L}$ Range	ξ Range
5.6	14	0 to 0.9	0.025 to 0.40
10	14	↕	0.050 to 0.40
15	14	↕	↕
10	8	↕	↕
10	20	0 to 0.9	0.050 to 0.40

It should be noted that the G. E. program does not account for the contribution of the portion of the nose forward of the starting characteristic for the unsteady solution, see Fig. 7. The contribution of this portion of the body was calculated using the Newtonian theory developed by Fisher[17], which for moderate bluntness and slender cones can be approximated by

$$C_{m_\alpha} = \frac{x'_{cg}}{\ell} \xi^2 H^2 \qquad (10)$$

$$C_{m_q} = -\left(\frac{x'_{cg}}{\ell}\right)^2 \xi^2 H^2 \qquad (11)$$

where

$$H = \frac{\ell'}{r}\left(2 - \frac{\ell'}{r}\right)$$

The nose contribution is small for moderate nose bluntness, $\xi < 0.15$, and becomes more important as nose bluntness is increased.

Figs. 8a and 8b show the results of these calculations for a 10° cone, at Mach 14, with various nose bluntness ratios, ξ, and for different locations of the moment reference center, x_{cg}/L. For $\xi = 0.05$, the center of pressure is at the station $x/L = 2/3$, and the value of x_{cg}/L for minimum damping is 3/4. Increasing the nose bluntness ratio moves the C. P. toward the base at first and then in forward direction. The moment center for minimum damping, however, steadily moves in forward direction, when ξ increases.

Figs. 9a and 9b are cross plots of these calculations for $x_{cg}/L = 0.4$, 0.5, and 0.6 with the correlation parameter C used as abscissa. The center of gravity location is seen to have little effect on the characteristic shape of the curves. Increasing nose bluntness leads to a deterioration of the damping derivatives beginning at $C \approx 0.9$. At $C \approx 0.6$, the damping derivatives reach minimum values, which are very close to zero. The static derivatives improve at first and reach peak values at $C \approx 0.7$. Further decrease of C leads to a drastic reduction of C_{m_α} also.

In Figs. 10a and 10b are shown the results of these calculations for C_{m_α} and $(C_{m_q} + C_{m_{\dot\alpha}})$ for the 5.6°, 10°, and 15° cones at M = 14 and with $(x_{cg}/L) = 0.5$. The characteristic behavior is the same for all cones. The only region where cone angle has any significant influence on C_{m_α} is for $0.6 < C < 0.8$. Here we see that C_{m_α} increases with cone angle. This trend is also present in the experimental data. The curves for $(C_{m_q} + C_{m_{\dot\alpha}})$ show that in general the

influence of nose bluntness on $(C_{m_q} + C_{m_{\dot{\alpha}}})$ is the same for all cone angles. For $C > 0.8$ these calculations show that $(C_{m_q} + C_{m_{\dot{\alpha}}})$ increases with cone angle; this is also verified by experiment, Figs. 5b and 6b.

The influence of Mach number is shown in Figs. 11a and 11b. Here, we have plotted the calculated C_{m_α} and $(C_{m_q} + C_{m_{\dot{\alpha}}})$ for the 10° cone with $(x_{cg}/L) = 0.5$ and for 3 different Mach numbers. These results indicate that, above Mach 14, Mach number has little influence on either C_{m_α} or $(C_{m_q} + C_{m_{\dot{\alpha}}})$, but below Mach 14, Mach number does influence the stability derivatives. The results for Mach 8 indicate that for lower Mach numbers the adverse effect of increasing the nose bluntness on $(C_{m_q} + C_{m_{\dot{\alpha}}})$ is not as severe as for higher Mach numbers. Fig. 12 shows a plot of $(C_{m_q} + C_{m_{\dot{\alpha}}})$ vs Mach number for a 10° cone with $\xi = 0.2$ and $(x_{cg}/L) = 0.55$; included are experimental results from Ref. 18 and from present tests. The calculations are qualitatively in agreement with experiment, showing that for this bluntness ratio the damping decreases with increased Mach number. Note that the experimental values are higher than those calculated.

CONCLUSION

Wind tunnel tests with air at Mach 14 and three different types of analyses agree in describing the high Mach number effect of nose blunting on the static and dynamic stability derivatives in pitch for spherically blunted slender cones at zero trim angle of attack. Using the cone angle-bluntness ratio correlation parameter $C = \sqrt{\Theta_c(1-\xi)/2\xi}$, it is shown that $C_{m_q} + C_{m_{\dot{\alpha}}}$ starts to deteriorate when C decreases below the value of one and reaches a minimum value at $C \approx 0.6$. The static stability, however, is improved at first and reaches a peak value at $C \approx 0.7$. Further decrease of C leads to a deterioration of C_{m_α} also.

REFERENCES

1. Walchner, O. and Clay, J. T., "Hypersonic Stability Derivatives of Blunted Slender Cones," AIAA Journal, Vol. 3, No. 4, p. 752, (April 1965).

2. Walchner, O. and Clay, J. T., "Nose Bluntness Effects on the Stability Derivatives of Slender Cones," Transactions of the Second Technical Workshop on Dynamic Stability Testing (Sponsored by AEDC and ARO, Inc.), Vol. I, Paper 8, (1965).

3. Quinn, B. P., "Blast Wave Effects on the Pitching of Blunt Cones," Proceedings of the 13th Annual Air Force Science and Engineering Symposium, Vol. II, Paper 37, (1966).

4. Chernyi, G. G., "Introduction to Hypersonic Flow," Translated by R. F. Probstein, Academic Press, New York, (1961).

5. Cheng, H. K., "Hypersonic Flow with Combined Leading Edge Bluntness and Boundary Layer Displacement Effect," Cornell Aeronautical Laboratory Report No. AF-1285-A-4, (August 1960).

6. Griffith, B. J. and Lewis, C. H., "A Study of Laminar Heat Transfer to Spherically Blunted Cones and Hemisphere-Cylinders at Hypersonic Conditions," AEDC TDR 63-102, (June 1963).

7. Marshall, L. A., "Hypersonic Dynamic Stability, Part I Summary," FDL-TDR-64-149, Part I, (January 1967).

8. Hobbs, R. B., Jr., "Hypersonic Dynamic Stability, Part II, Conical Body Experimental Program," FDL-TDR-64-149, Part II, (January 1967).

9. Rie, H., Linkiewicz, E. A., and Bosworth, F. D., "Hypersonic Dynamic Stability, Part III, Unsteady Flow Field Program," FDL-TDR-64-149, Part III, (January 1967).

10. Walchner, O., Sawyer, F., Quinn, B., and Friberg, E., "Hypersonic Stability Derivatives for a Standard 10 Degree Cone," ARL 67-0099, (May 1967).

11. Gregorek, G. M., and Lee, J. D., "Design Performance and Operational Characteristics of the ARL Twenty-Inch Hypersonic Wind Tunnel," ARL 62-392, (August 1962).

12. Gregorek, G. M., "Initial Calibration and Performance of the ARL Twenty-Inch Hypersonic Wind Tunnel," ARL 62-393, (August 1962).

13. Tepe, F. R., Jr., Brown, D. L., Token, K. H., and Hollmer, W., "Theoretical Operating Ranges and Calibration Results of the ARL Twenty-Inch Hypersonic Wind Tunnel," ARL 63-189, (September 1965).

14. Daum, F. L., "Air Condensation in a Hypersonic Wind Tunnel," AIAA Journal, Vol. 1, No. 5, pp. 1043-1046, (May 1963).

15. Goddard, R. T., "Observed Supersaturation in the ARL Twenty-Inch Hypersonic Wind Tunnel," ARL 65-214, (October 1965).

16. Walchner, O., Sawyer, F. M., and Koob, S. J., "Dynamic Stability Testing in a Mach 14 Blow Down Wind Tunnel," Journal of Spacecraft and Rockets, Vol. 1, No. 4, pp. 433, (July-August 1964).

17. Fisher, L. R., "Equations and Charts for Determining the Hypersonic Stability Derivatives of Combinations of Cone Frustums Computed by Newtonian Impact Theory," NASA TN D-149, (November 1959).

18. Preslin, R. H., "High Amplitude Dynamic-Stability Characteristics of Blunt 10-Degree Cones," JTL Technical Report No. 32-1012, (October 1966).

19. Tobak, M. and Wehrand, W. R., "Stability Derivatives of Cones at Supersonic Speeds," NACA TN 3788, (September 1956).

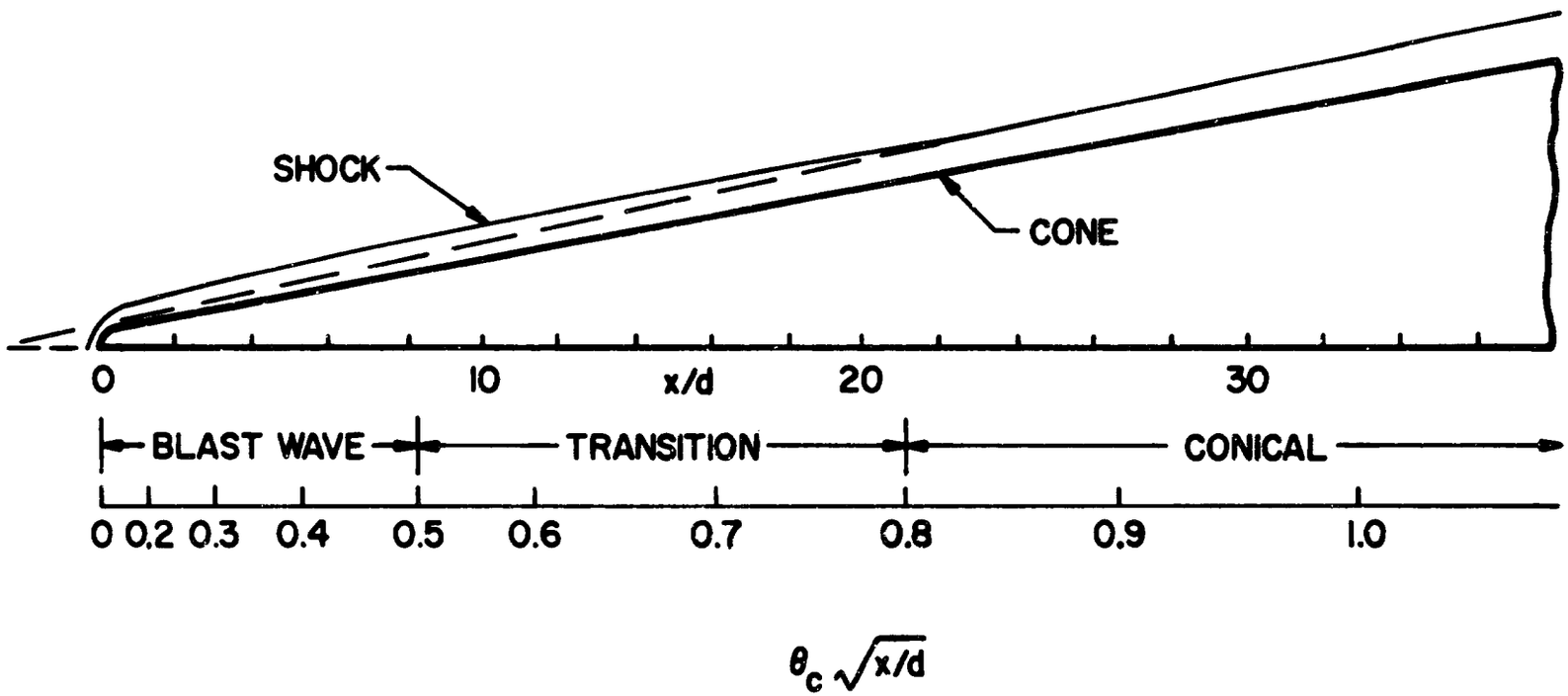

Fig. 1 Flow Regimes for a 10° Half Angle Cone

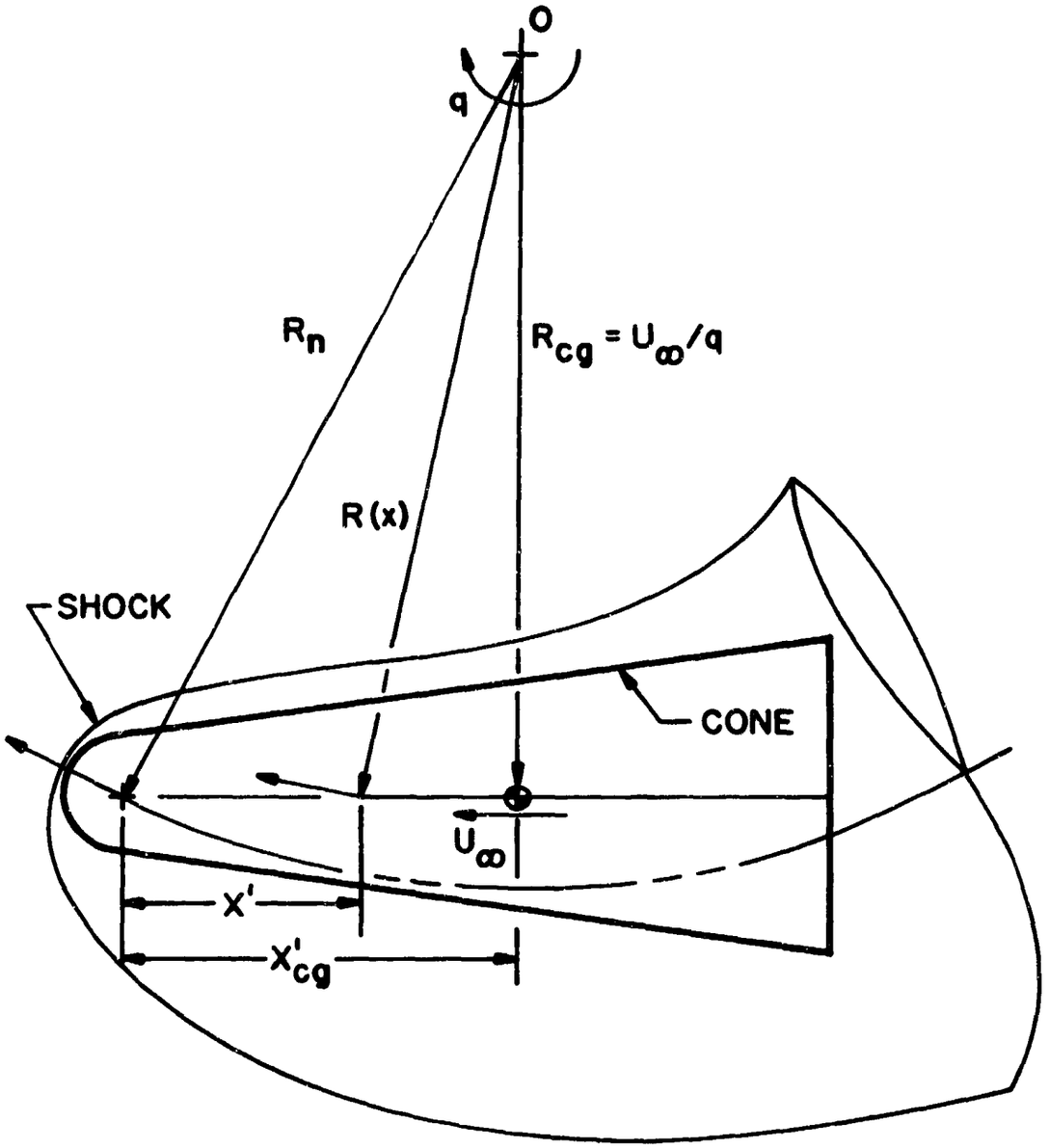

Fig. 2a Rotating Blunt Cone, $C \leq 0.5$

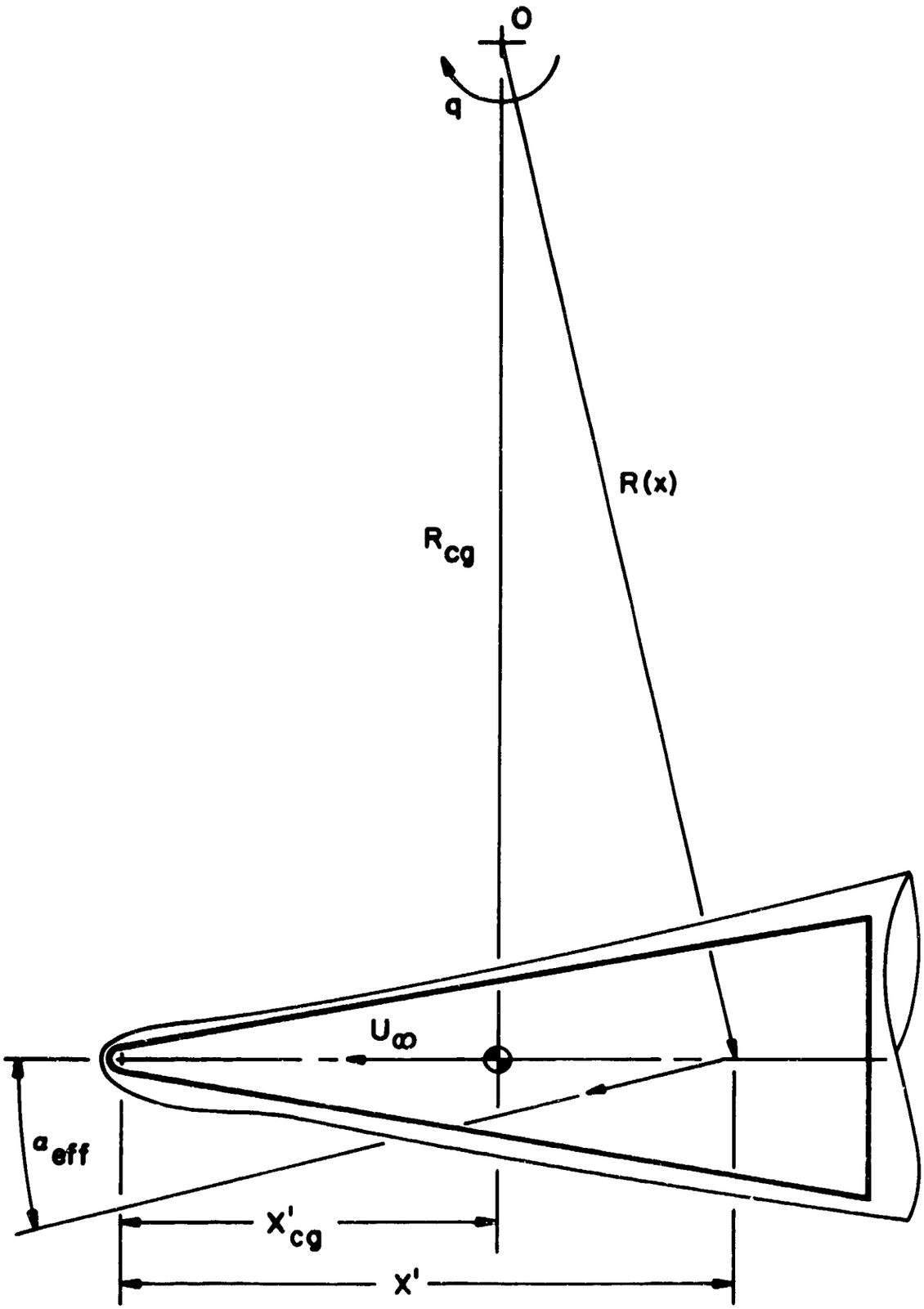

Fig. 2b Rotating Blunt Cone, $C \geq 1.0$

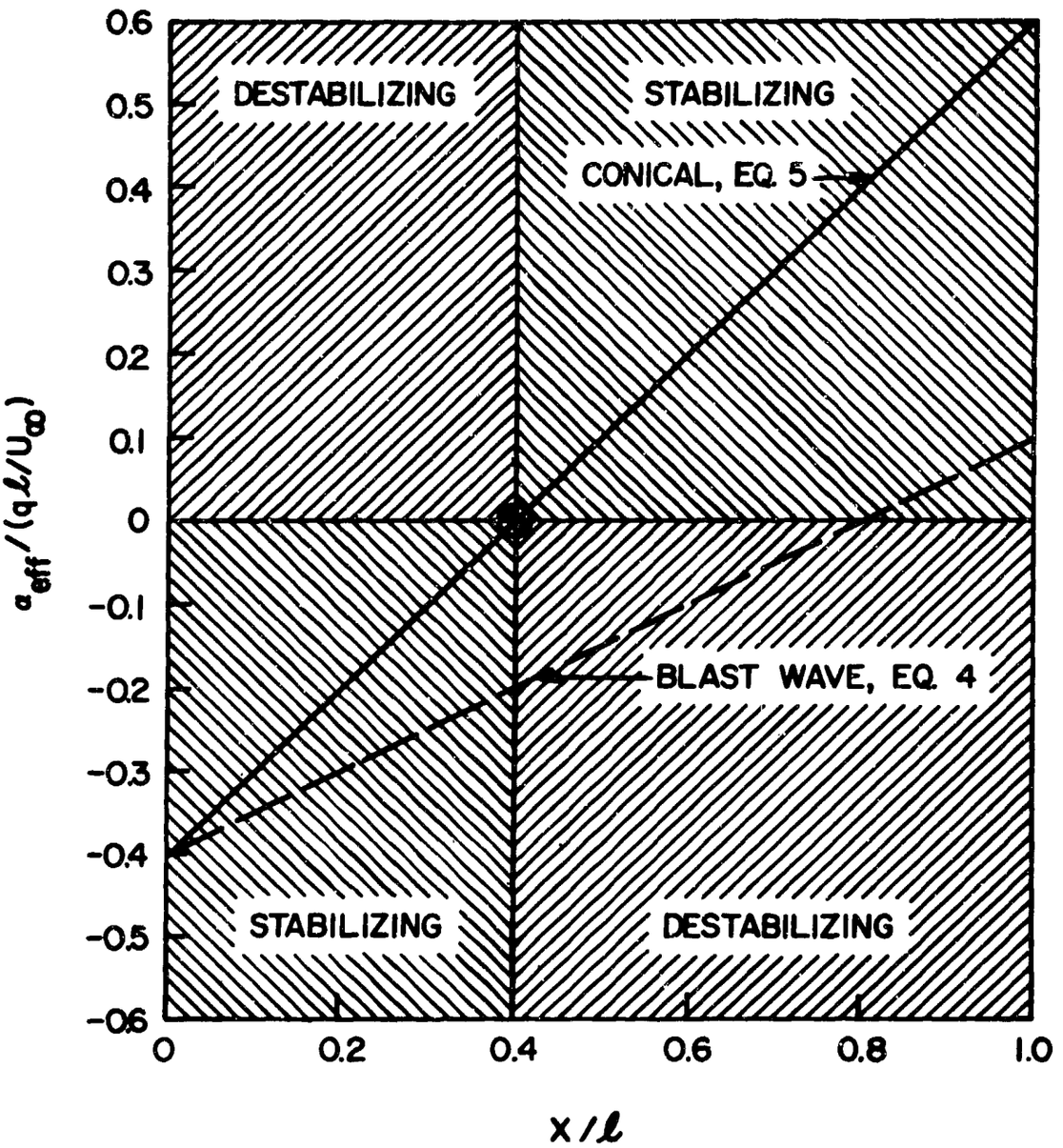

Fig. 3 Effective Angle of Attack Per Unit Reduced Frequency vs Body Station for Blast Wave and Conical Type Flows, $\frac{x'_{cg}}{\ell} = 0.4$

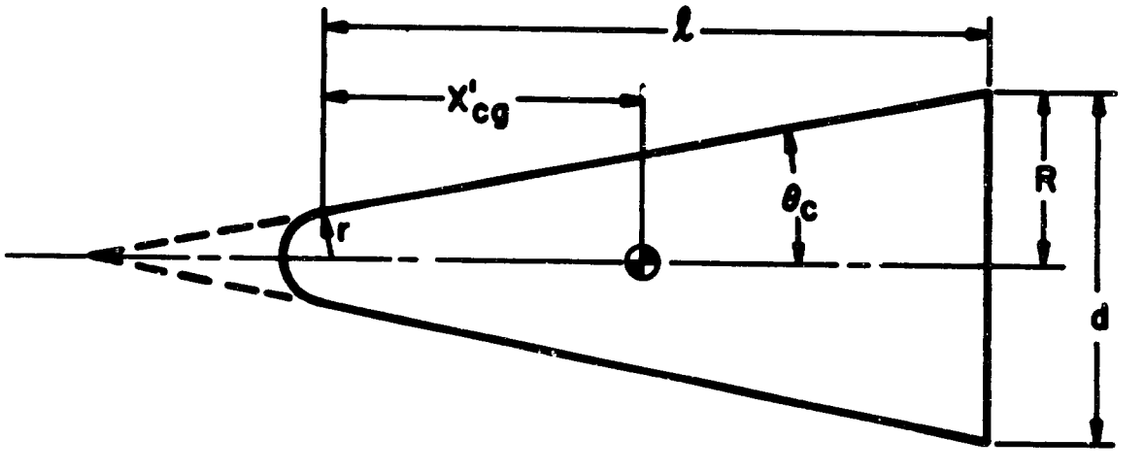

θ_c	5.6° (REF. 2)			10°		
$(\ell - X'_{cg})$	2.045d			1.112d		
NOSE	ξ	X'_{cg}/ℓ	$C=\left[\theta_c(1-\xi)/2\xi\right]^{1/2}$	ξ	X'_{cg}/ℓ	$C=\left[\theta_c(1-\xi)/2\xi\right]^{1/2}$
I	0.0039	0.597	3.520	0.025	0.593	1.848
II	0.0257	0.588	1.360	0.050	0.583	1.290
III	0.0495	0.577	0.968	0.075	0.573	1.039
IV	0.0988	0.555	0.668	0.100	0.560	0.887
V	0.1983	0.500	0.444	0.150	0.535	0.704
VI	0.2970	0.431	0.340	0.200	0.506	0.591
VII	———	———	———	0.300	0.437	0.452

Fig. 4 Test Configurations

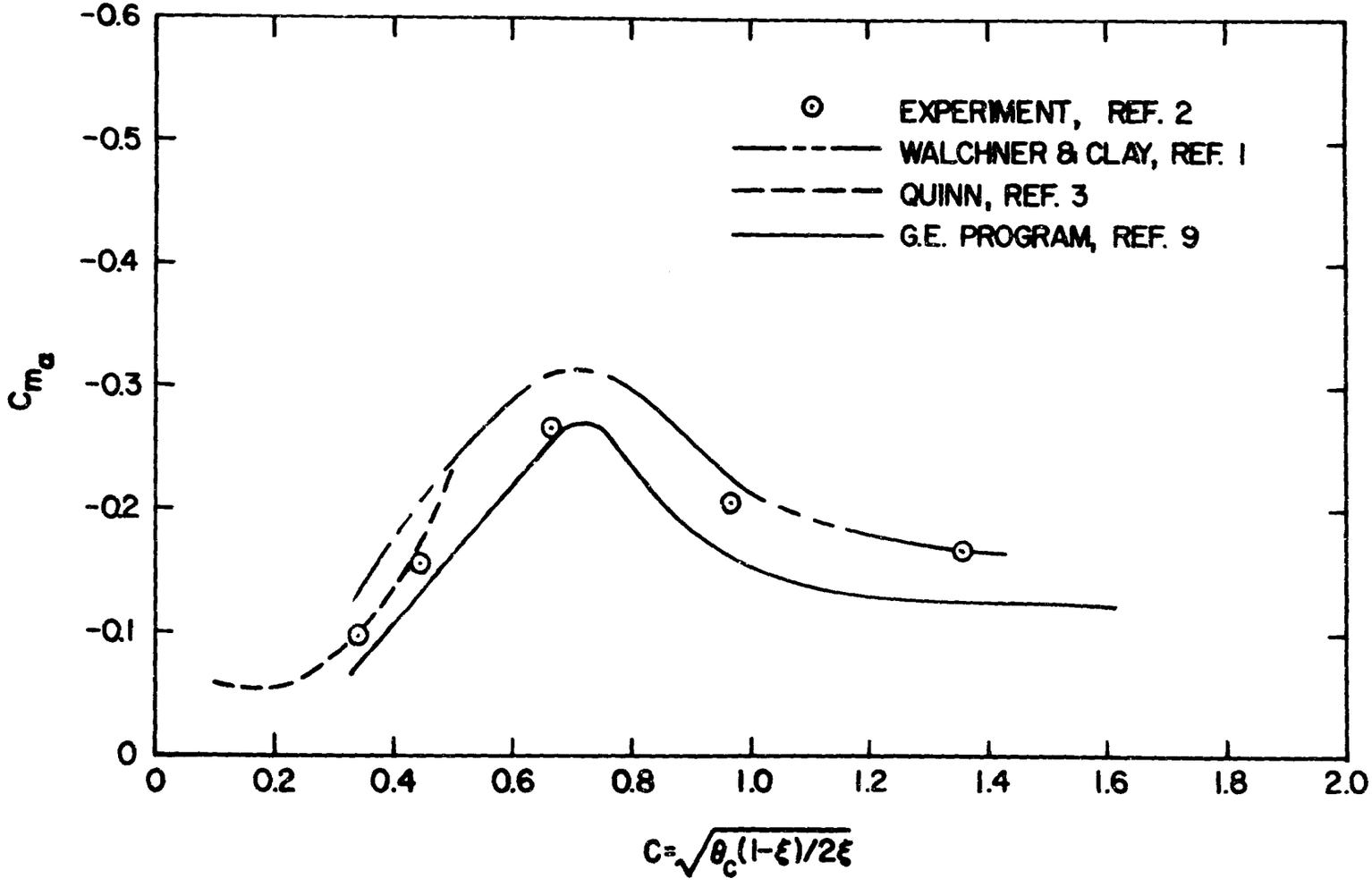

Fig. 5a Static Pitching Moment Derivative, C_{m_α}, vs Correlation Parameter for a 5.6° Cone, $M_\infty \approx 14.14, R_{e_{\infty_L}} = .4\times10^6 - .6\times10^6$

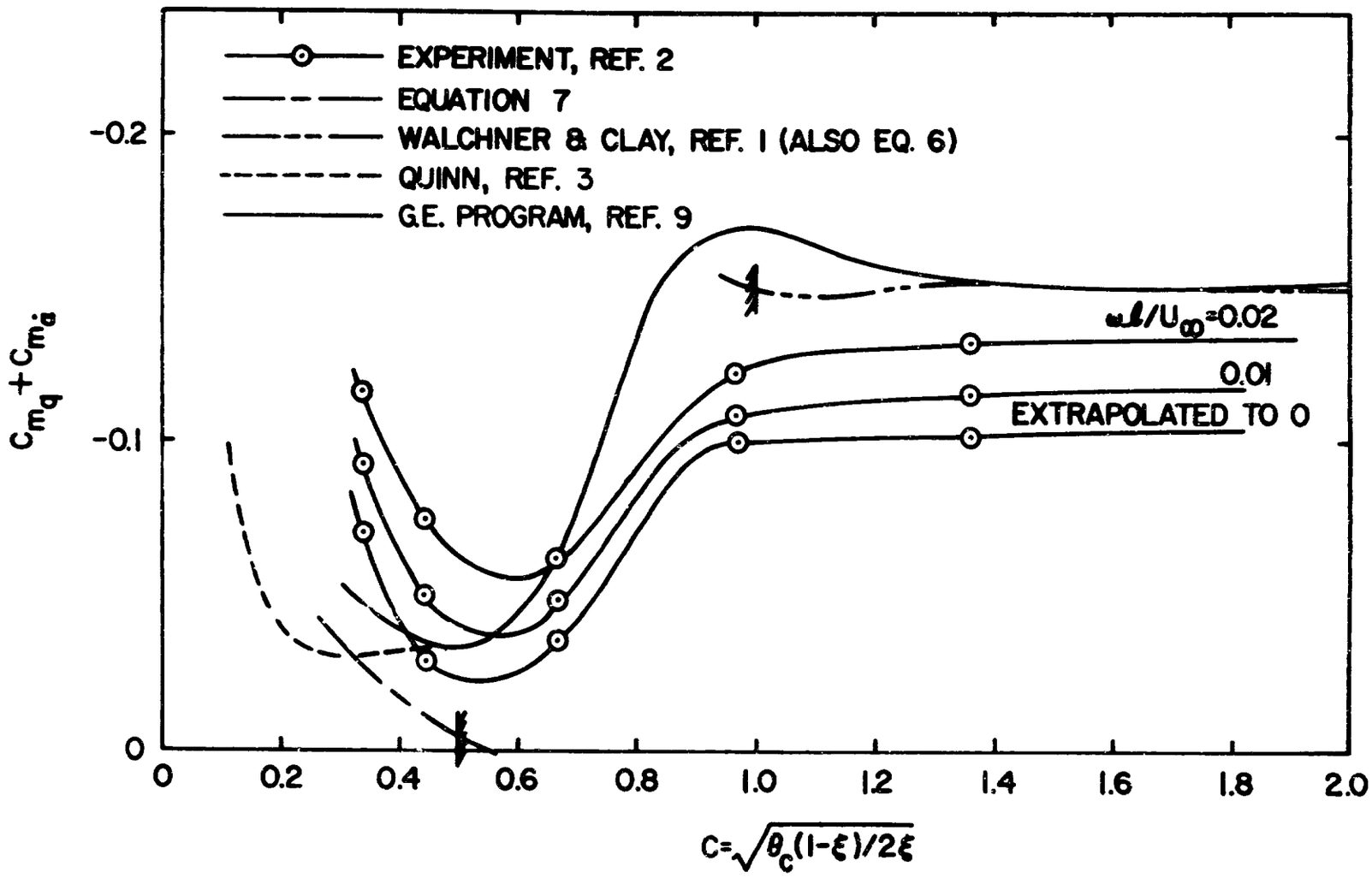

Fig. 5b Damping Moment Derivatives, $(C_{m_q} + C_{m_{\dot\alpha}})$, vs Correlation Parameter for a 5.6° Cone, $M_\infty \approx 14.14$

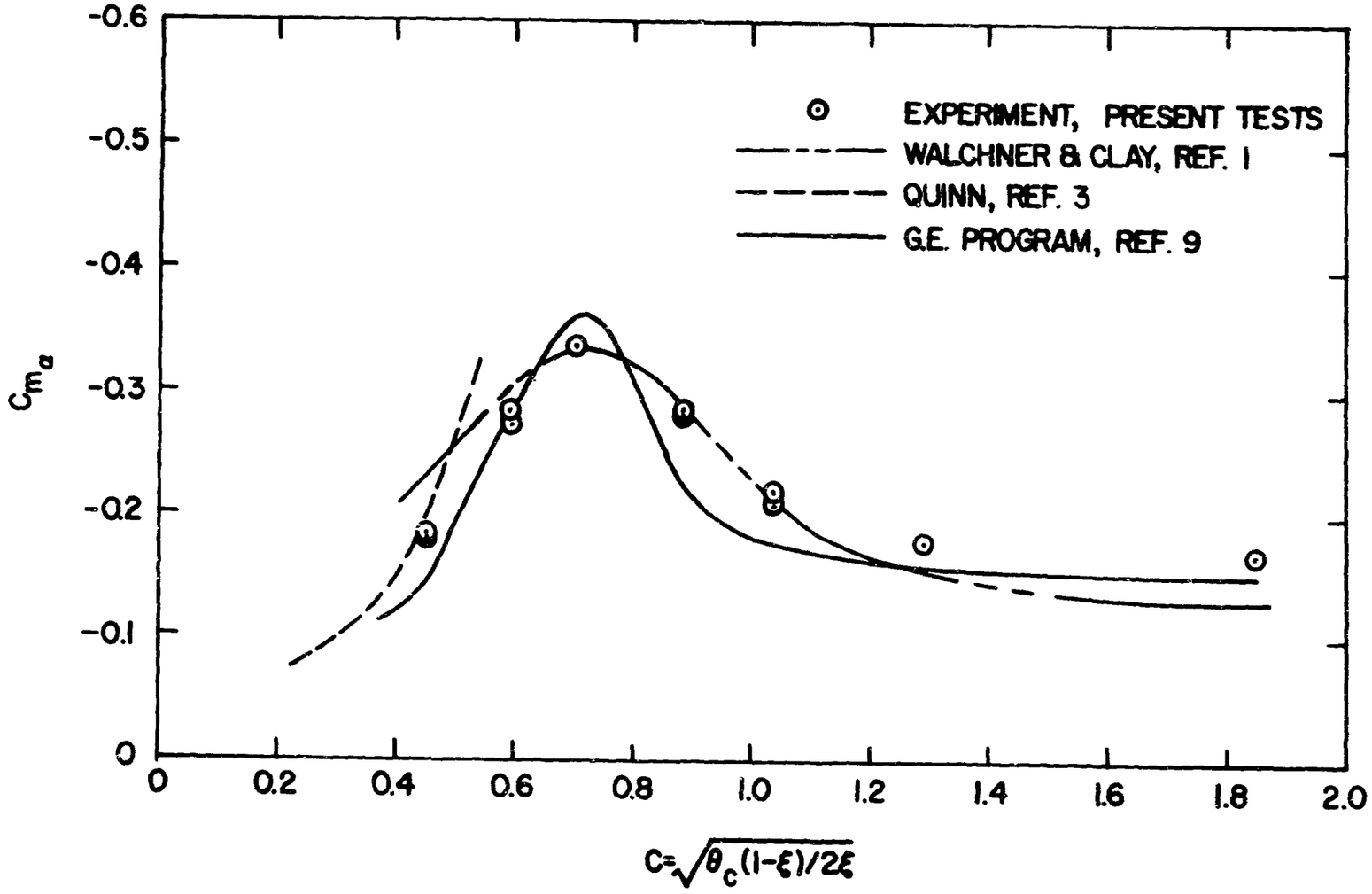

Fig. 6a Static Pitching Moment Derivative, C_{m_α}, vs Correlation Parameter for 10° Cone, $M_\infty \approx 14.2$, $\omega L/U_\infty = .0154$-$.0186$, $R_{e_{\infty_L}} = .42 \times 10^6$ - $.55 \times 10^6$

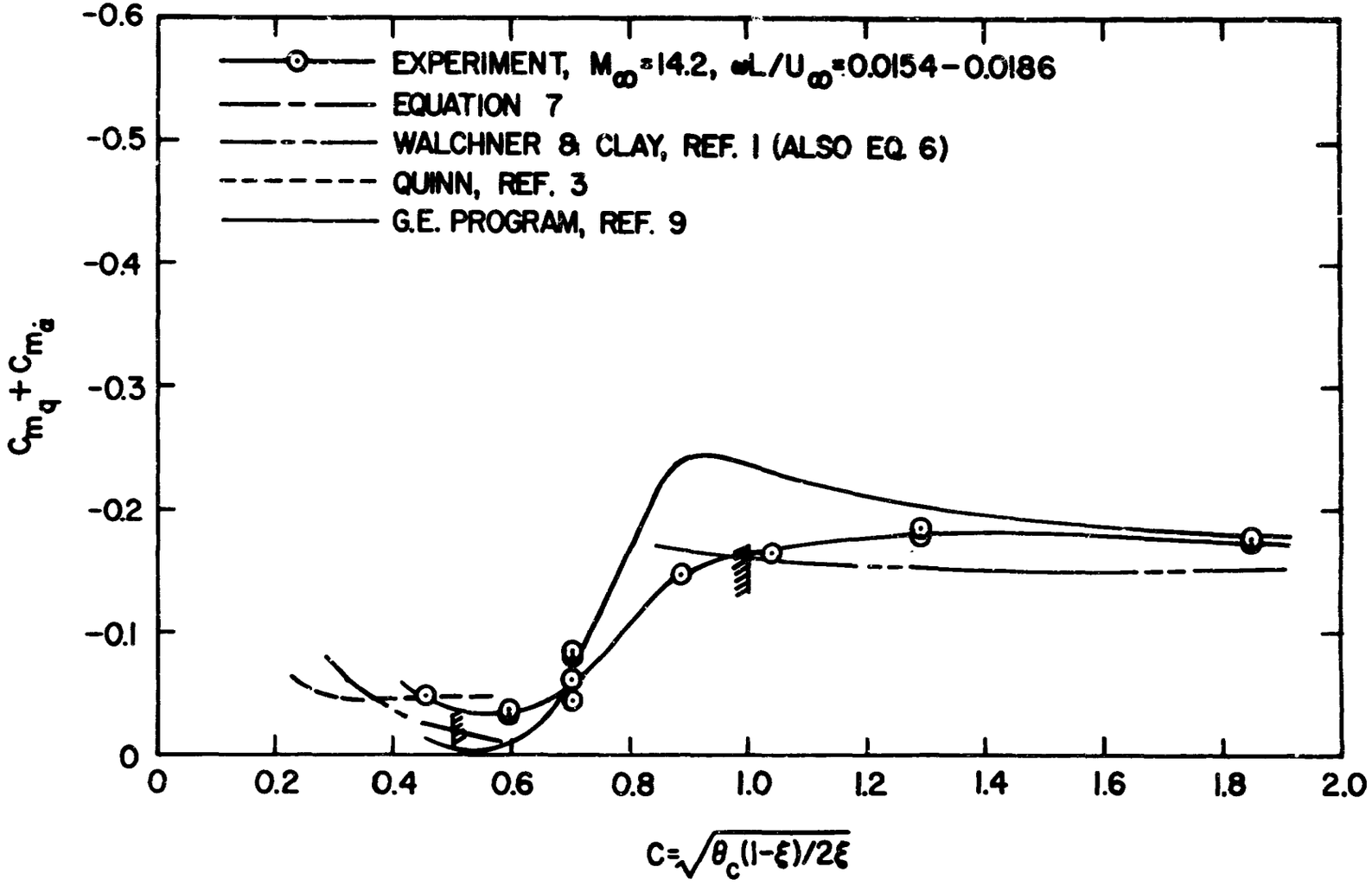

Fig. 6b Damping Moment Derivatives, $(C_{m_q} + C_{m_{\dot{\alpha}}})$ vs Correlation Parameter for 10° Cone

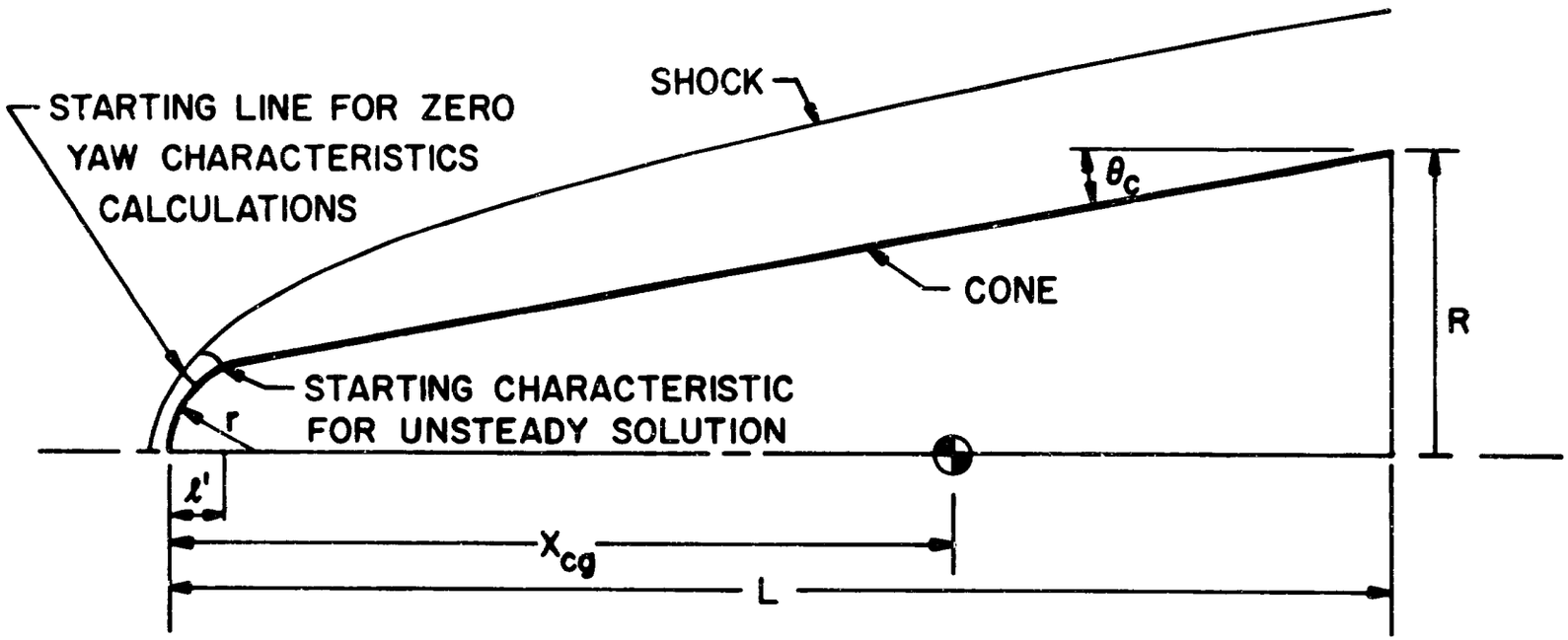

Fig. 7 Cone Geometry and Definitions for Characteristics Solution

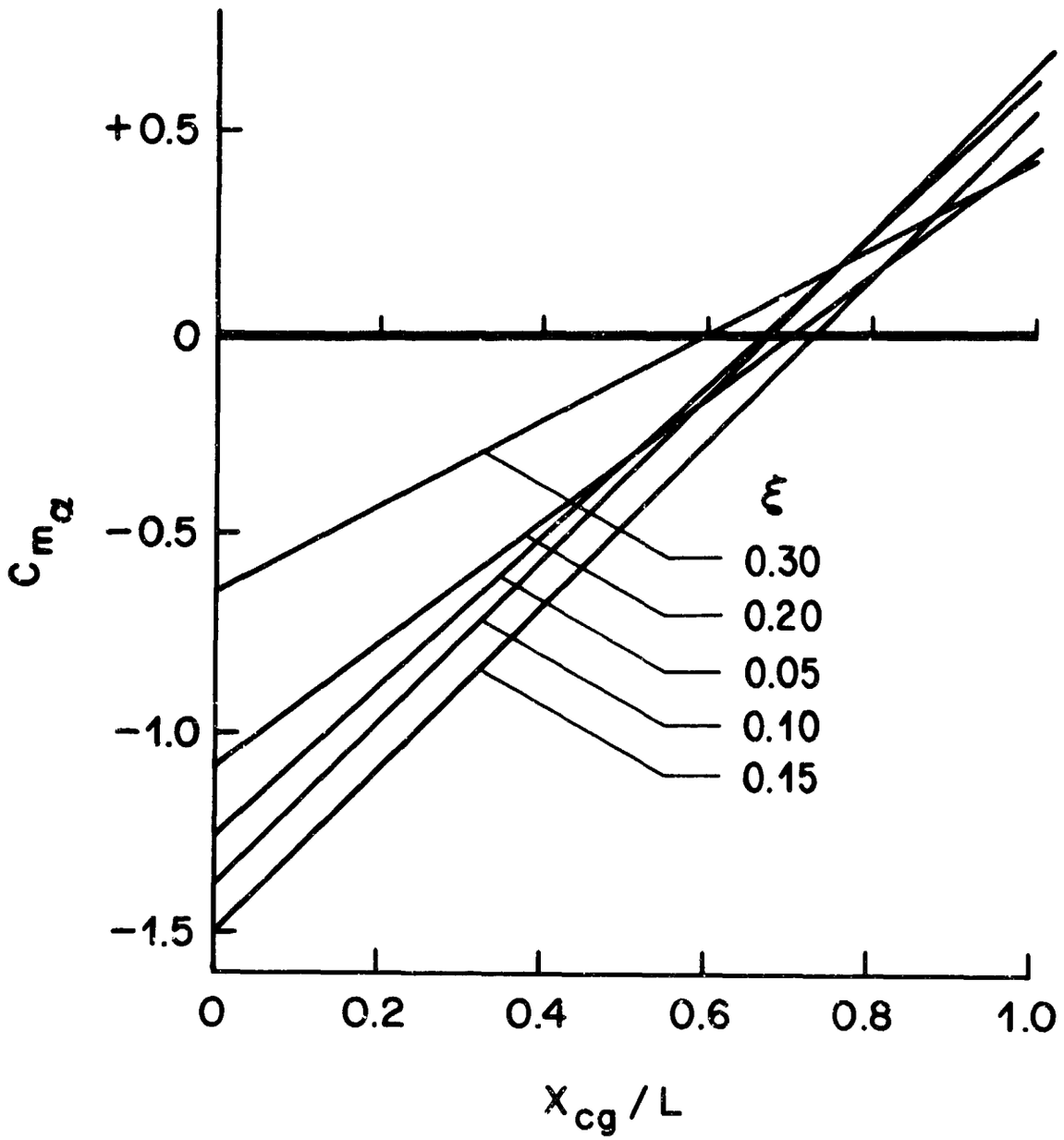

Fig. 8a Calculated Static Pitching Moment Derivatives, C_{m_α}, for Various Bluntness Ratios, ξ, vs x_{cg}/L. $\Theta_c = 10°$, M = 14, G. E. Program

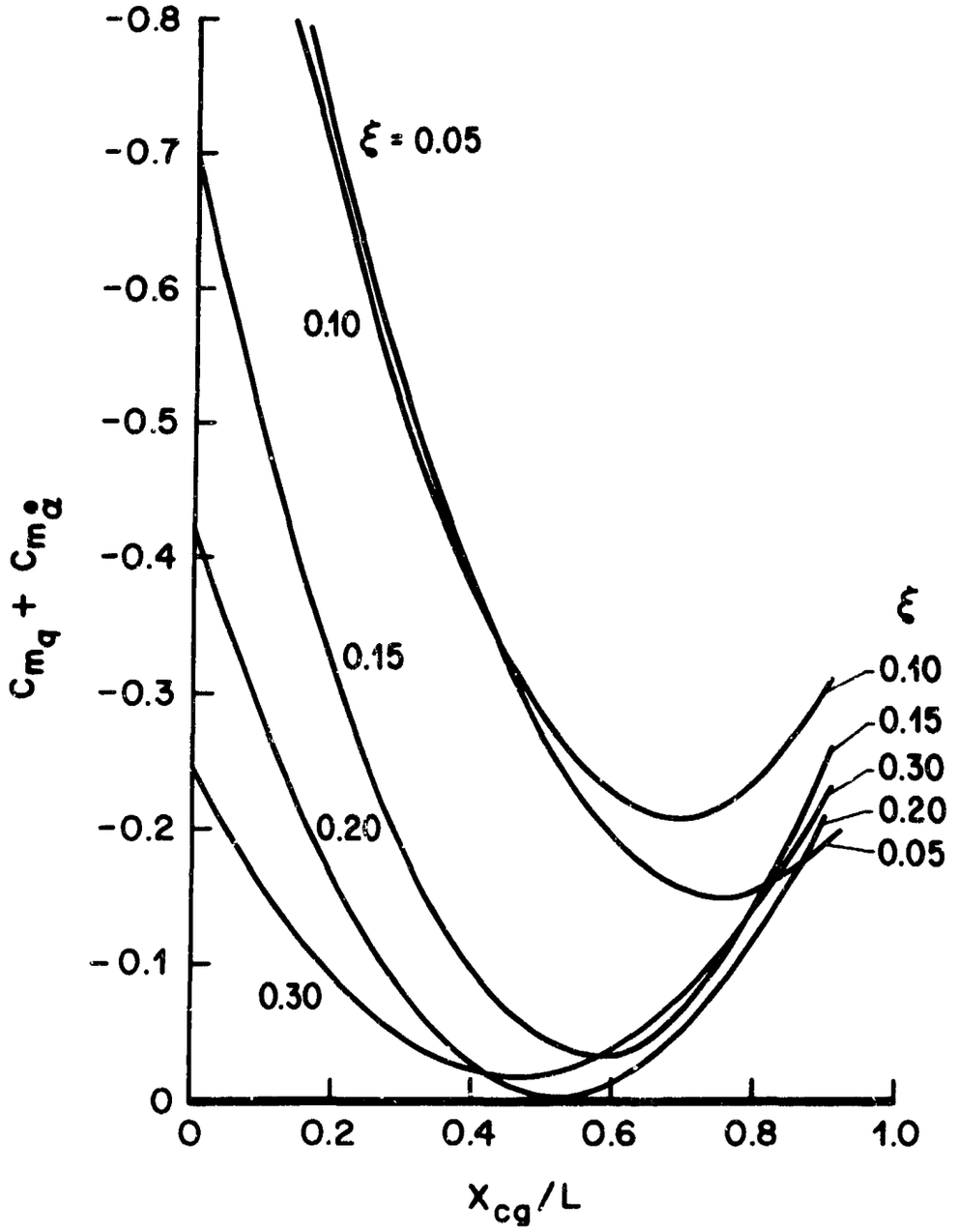

Fig. 8b Calculated Damping Derivatives, $C_{m_q} + C_{m_{\dot{\alpha}}}$, for Various Bluntness Ratios, ξ, vs x_{cg}/L. $\Theta_c = 10°$, M = 14, G. E. Program

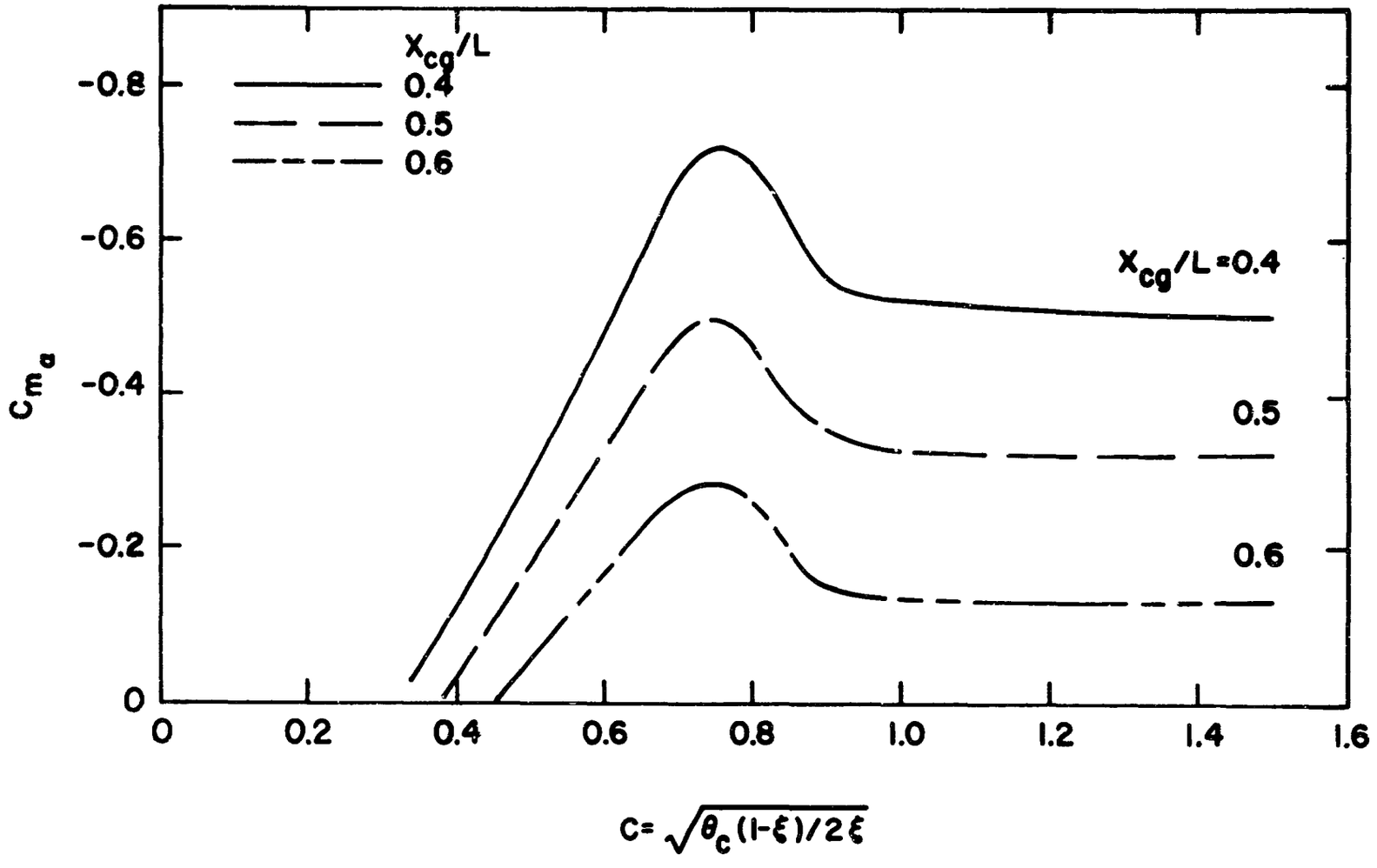

Fig. 9a Calculated Static Pitching Moment Derivative, C_{m_α}, vs Correlation Parameter for 10° Cone at M = 14 for Various c.g. Locations, G. E. Program

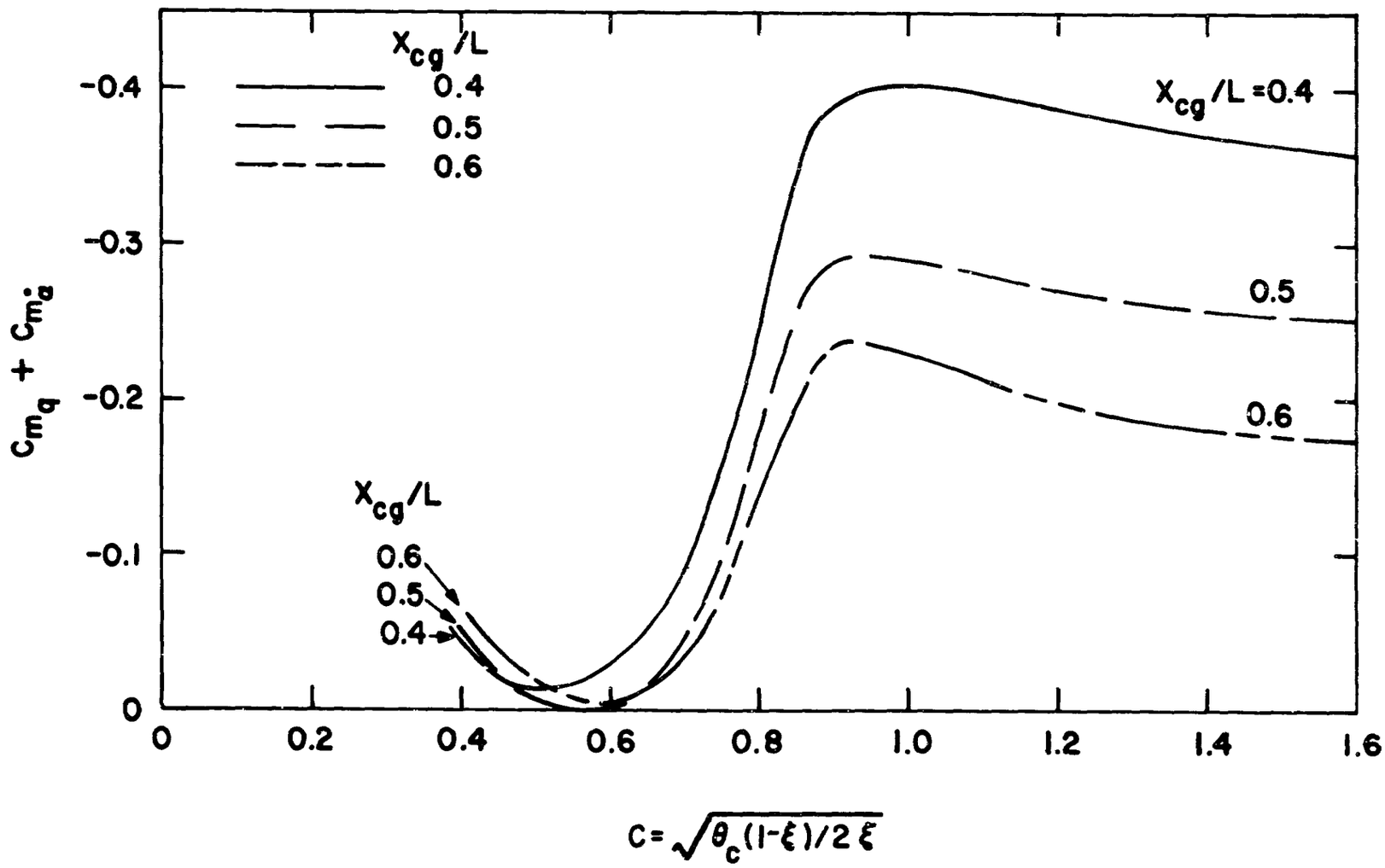

Fig. 9b Calculated Damping Moment Derivatives, ($C_{m_q} + C_{m_{\dot{\alpha}}}$) vs Correlation Parameter for 10° Cone at M = 14 for Various c.g. Locations, G. E. Program

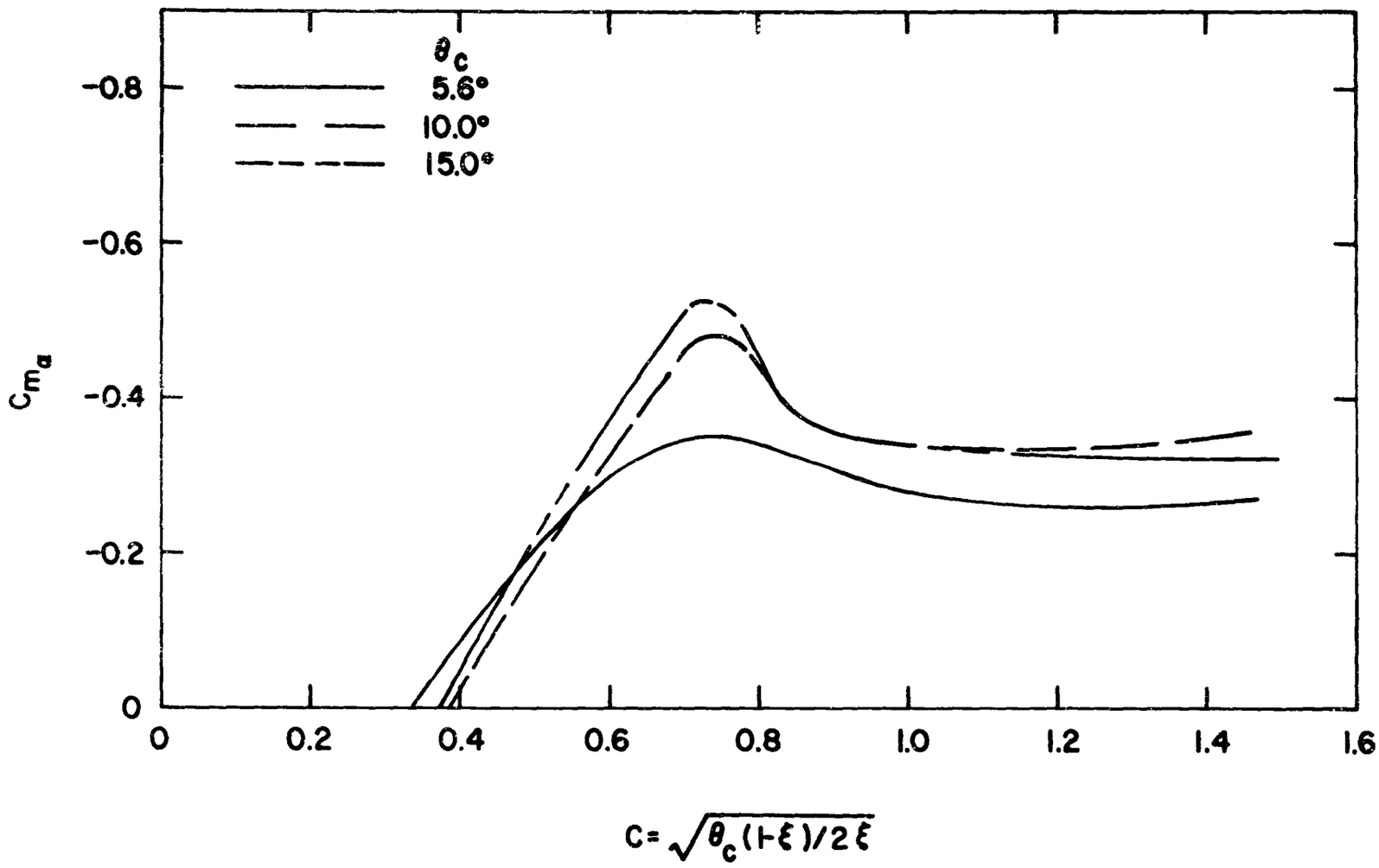

Fig. 10a Calculated Static Pitching Moment Derivative, C_{m_α}, vs Correlation Parameter for 5.6°, 10°, and 15° Cones at M = 14 for $\frac{x_{cg}}{L} = 0.5$, G. E. Program

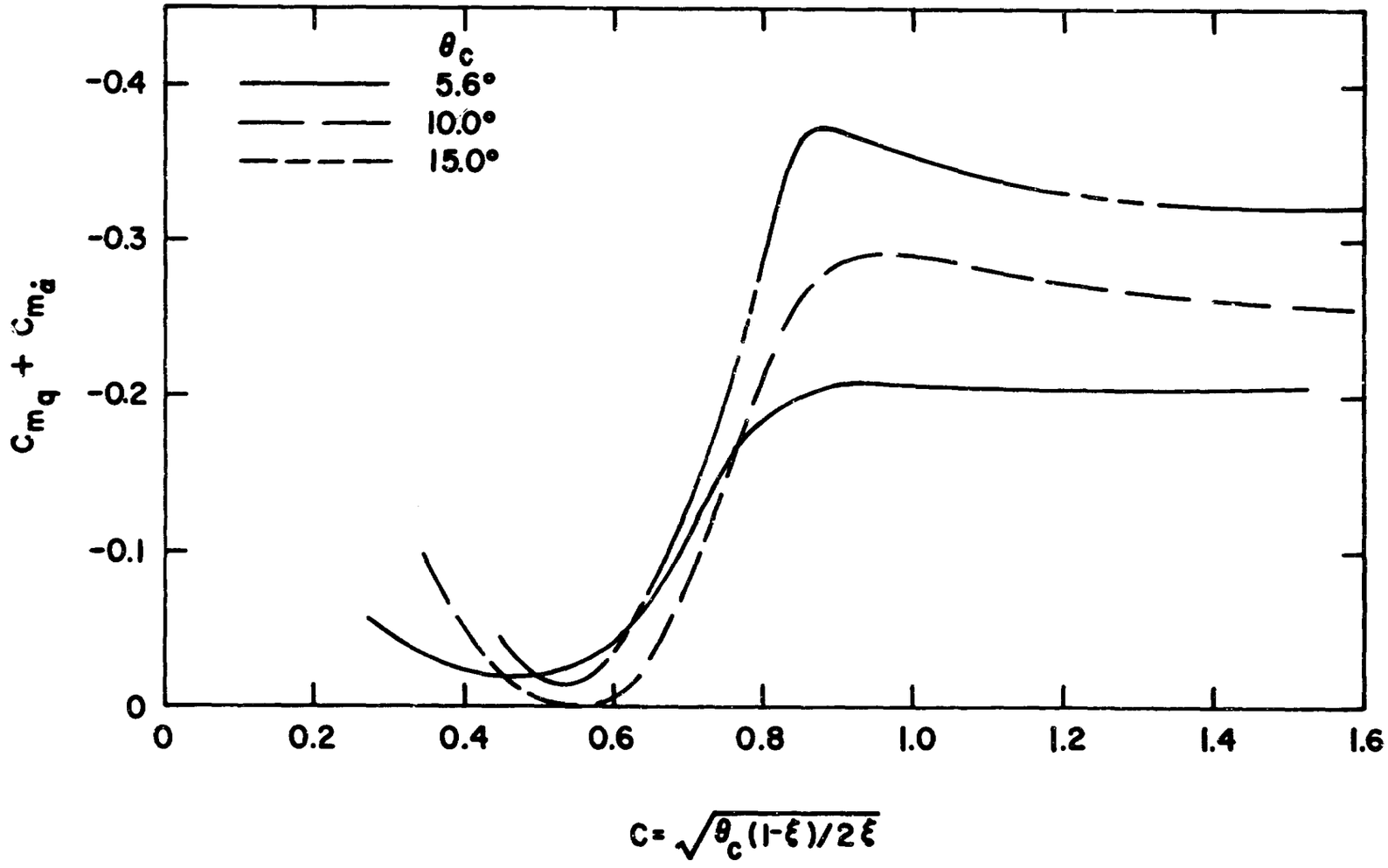

Fig. 10b Calculated Damping Moment Derivatives, $(C_{m_q} + C_{m_{\dot{\alpha}}})$, vs Correlation Parameter for 5.6°, 10°, and 15° Cones at M = 14 for $\frac{x_{cg}}{L} = 0.5$, G. E. Program

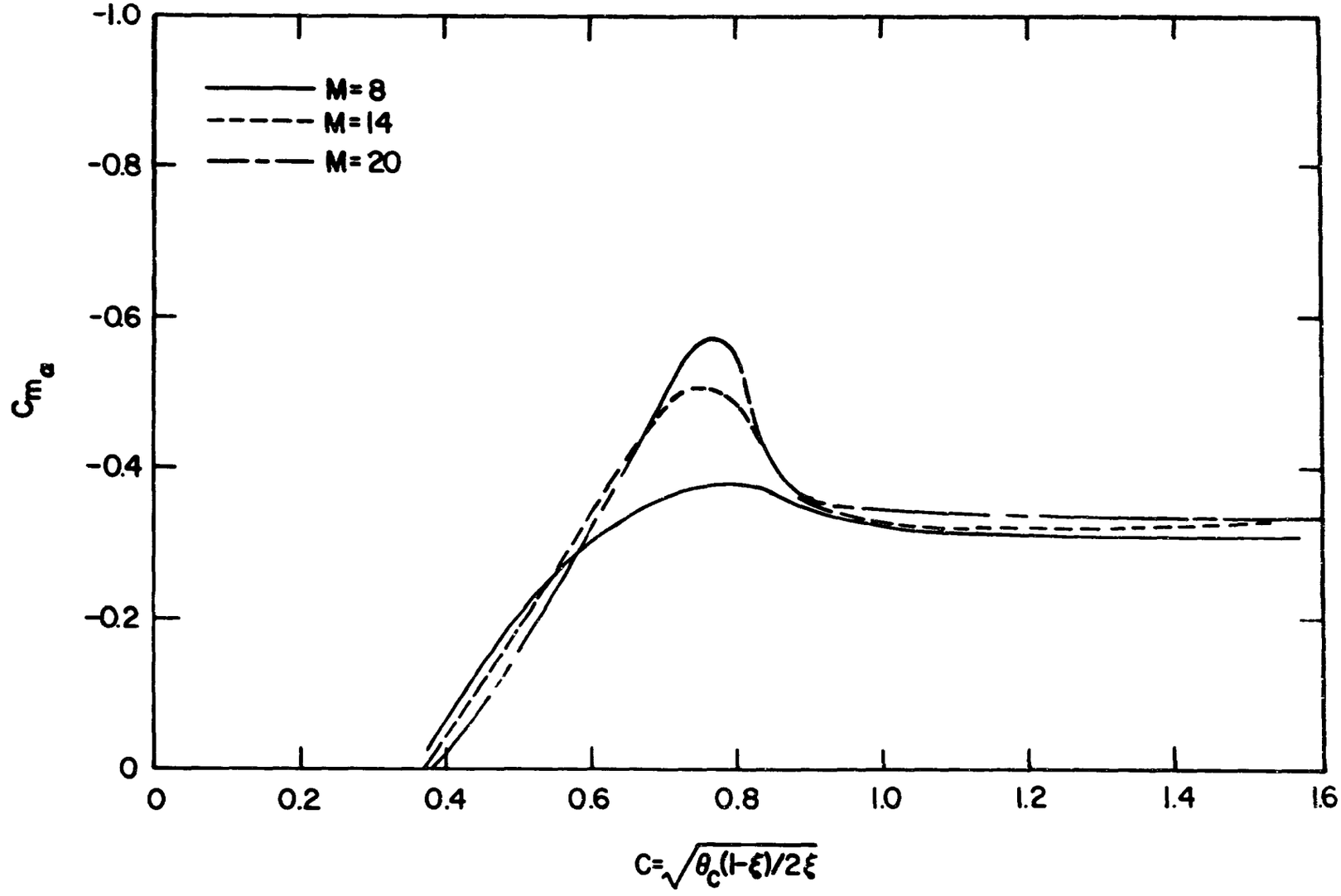

Fig. 11a Calculated Pitching Moment Derivative, C_{m_α}, vs Correlation Parameter for 10° Cone at M_∞ = 8, 14, 20 for $\frac{x_{cg}}{L}$ = 0.5, G. E. Program

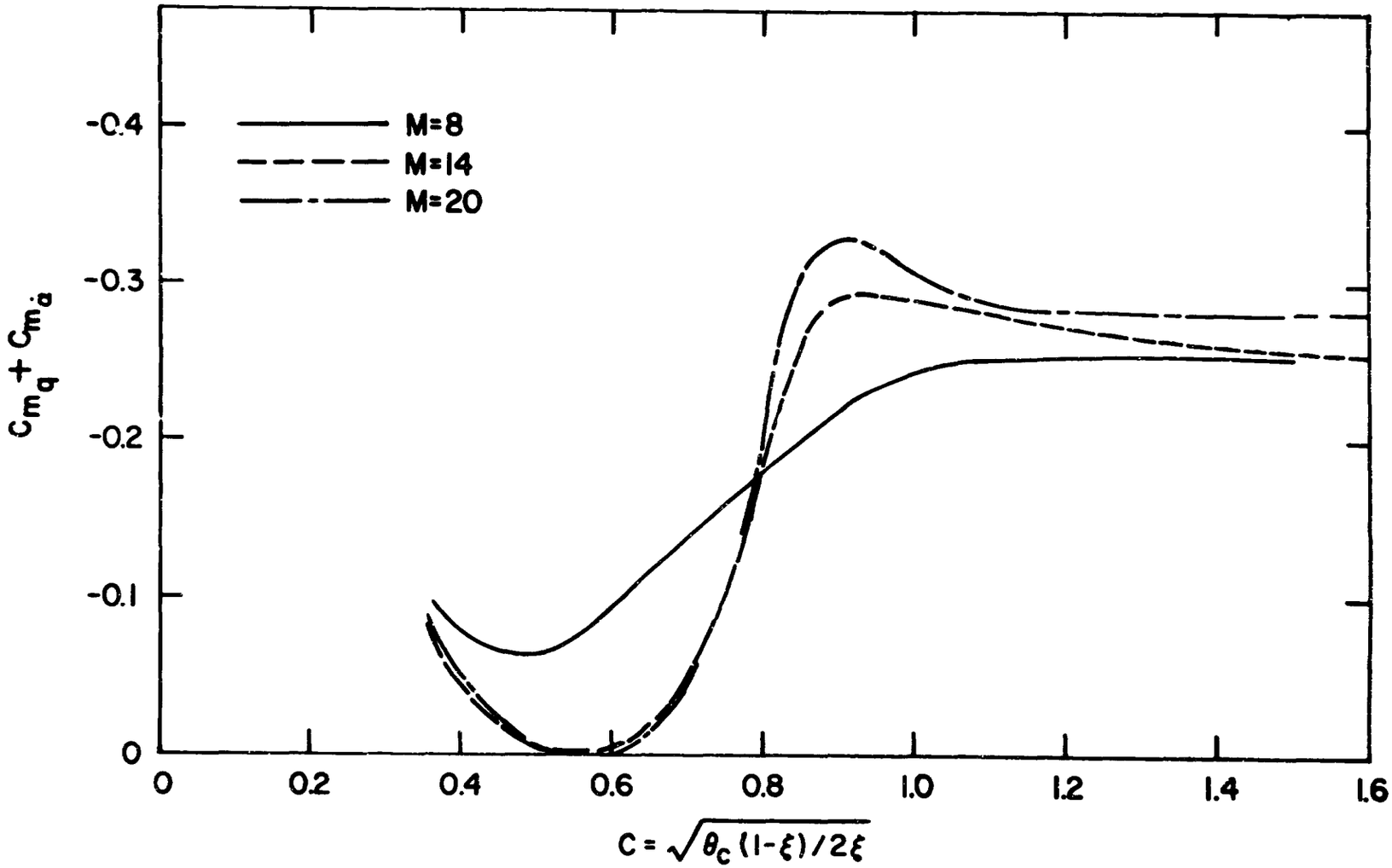

Fig. 11b Calculated Damping Moment Derivatives, $(C_{m_q} + C_{m_{\dot{\alpha}}})$, vs Correlation Parameter for 10° Cone at M_∞ = 8, 14, 20 for $\frac{x_{cg}}{L}$ = 0.5, G. E. Program

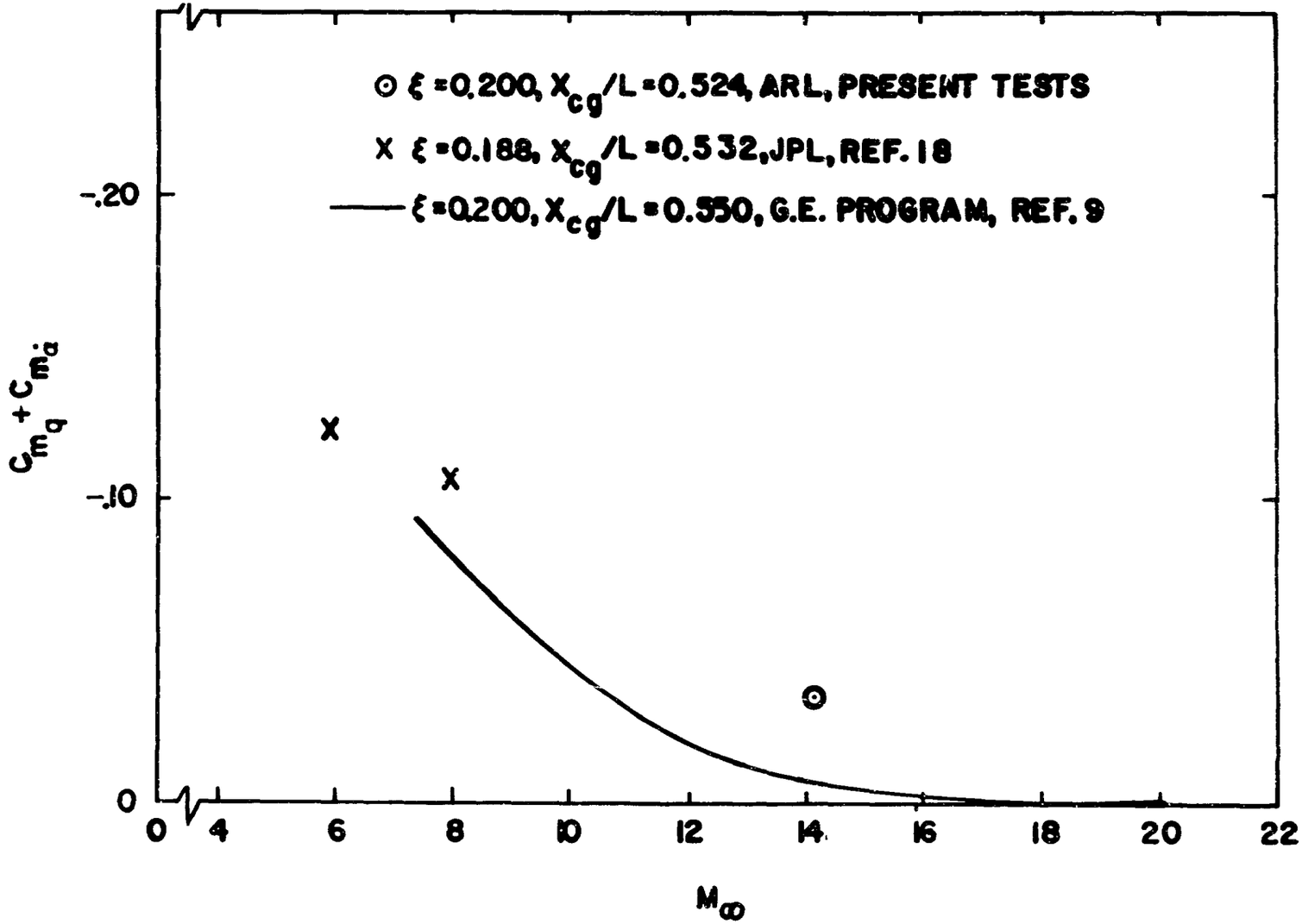

Fig. 12 Theoretical and Experimental Damping Moment Derivatives, $(C_{m_q} + C_{m_{\dot{\alpha}}})$, vs Free Stream Mach Number for a 10° Cone with Bluntness Ratio ≈ 0.2

Unclassified

Security Classification

DOCUMENT CONTROL DATA - R & D

(Security classification of title, body of abstract and indexing annotation must be entered when the overall report is classified)

1. ORIGINATING ACTIVITY (Corporate author) Aerospace Research Laboratories Hypersonic Research Laboratory Wright-Patterson AFB, Ohio 45433	2a. REPORT SECURITY CLASSIFICATION Unclassified 2b. GROUP

3. REPORT TITLE

Nose Bluntness, Cone Angle, and Mach Number Effects on the Stability Derivatives of Slender Cones

4. DESCRIPTIVE NOTES (Type of report and inclusive dates)

Scientific. Final.

5. AUTHOR(S) (First name, middle initial, last name)

James T. Clay

6. REPORT DATE	7a. TOTAL NO. OF PAGES	7b. NO. OF REFS
September 1967	43	19

8a. In-house research b. PROJECT NO. 7064-00-01 c. DoD Element 61445014 d. DoD Subelement 681307	9a. ORIGINATOR'S REPORT NUMBER(S) 9b. OTHER REPORT NO(S) (Any other numbers that may be assigned this report) ARL 67-0185

10. DISTRIBUTION STATEMENT

1. This document has been approved for public release and sale; its distribution is unlimited.

11. SUPPLEMENTARY NOTES	12. SPONSORING MILITARY ACTIVITY
TECH OTHER	Aerospace Research Laboratories (ARR) Wright-Patterson AFB Ohio 45433

13. ABSTRACT

A theoretical and experimental study to evaluate the influence of spherical nose bluntness, of cone angle, c.g. location and Mach number on the stability characteristics in pitch of blunt slender cones has been conducted at the USAF Aerospace Research Laboratories. A 10° half angle cone with nose bluntness ratios from .025 to .30 was investigated in the ARL 20" Hypersonic Wind Tunnel at M = 14. The small amplitude free oscillation technique was used to extract the static and dynamic stability derivatives from the time history of a planar oscillatory motion about zero trim angle of attack. The observed effect of the nose bluntness on the stability derivatives was quite similar to earlier results with a 5.6° half angle cone. Again, a severe breakdown of the damping derivatives was found for large bluntness ratios. An estimate of the pitch-induced angles of attack for large bluntness ratios was based on the physics of the blast wave type flow. It was found that these induced angles differ from those applicable for pointed cones or for small bluntness ratios where the flow has mainly conical character. The tangent cone method in connection with these different types of pitch-induced angles of attack qualitatively predicts the observed breakdown of the damping derivatives. A computer program designed by General Electric Corp. was used to compare the ARL test results with G. E.'s unsteady flow field theory. Reasonably good agreement was obtained. The G. E. program was also used to calculate the effects of cone angle, c.g. location, and Mach number on the stability derivatives of spherically blunted cones. The earlier derived parameter $C = \sqrt{\theta_c (1-\xi)/2\xi}$ was found, to correlate well the effect of nose blunting on the stability derivatives, (θ_c = cone half angle, ξ = nose radius/base radius).

DD FORM 1 NOV 65 1473

Unclassified

Security Classification

14. KEY WORDS	LINK A		LINK B		LINK C	
	ROLE	WT	ROLE	WT	ROLE	WT
Hypersonic						
Blunted cone						
Stability derivatives in pitch						